8552 *Inorg. Chem.* **2010**, *49*, 8552–8557
DOI: 10.1021/ic101165k

Inorganic Chemistry
Article

Rationally Designed Fluorescence Turn-On Sensors: A New Design Strategy Based on Orbital Control

Hyo Sung Jung,[†] Kyoung Chul Ko,[‡] Jae Hong Lee,[†] Sang Hoon Kim,[†] Sankarprasad Bhuniya,[†] Jin Yong Lee,*[,‡] Youngmee Kim,[§] Sung Jin Kim,[§] and Jong Seung Kim*[,†]

[†]*Department of Chemistry, Korea University, Seoul, 136-704, Korea,* [‡]*Department of Chemistry, Sungkyunkwan University, Suwon 440-746, Korea, and* [§]*Department of Chemistry and Division of Nano Sciences, Ewha Womans University, Seoul 120-750, Korea*

Received June 10, 2010

Herein, we explore a new strategy in the chemo-sensor field for fluorescence amplification upon binding with metal ions based on controlled participation of the nitrogen lone pair orbital. The basic architecture of the sensor entails a fluorophore, the sp^2 hybridized nitrogen lone pair (-C═N-), and a chelator site referred to as the control part. Though nonplanar and nonfluorescent, compound **IC1** achieved pseudo planarity from binding with Zn^{2+} as indicated by the increased fluorescence signal. Its other analogue (**IC2**) is also planar, and unlike **IC1**-Zn^{2+} was fluorescent with a lack of binding affinity to metal ions. The time-dependent density functional theory (TDDFT) calculations revealed that the fluorescence amplification was due to the blocking of the nitrogen lone pair orbital; unlikely geometrical rearrangements were insignificant. This could indicate a breakthrough concept in the future design of fluorescent turn-on sensors.

Introduction

Nature has created sophisticated machinery to control the activities of essential trace elements, which include enzymes, cofactors with catalytic functions, and structural support elements in human beings.[1,2] Since the nineteenth century, various efforts have been exerted to detect numerous essential, and indeed, toxic metal ions in biological, as well as in the natural, environment. Spawned from these efforts, fluorescent sensors offer better sensitivity, specificity, and real-time monitoring with fast response time over other chemosensors.[3] To date, a variety of fluorescent chemosensors have been reported pertaining to the signaling mechanisms of photo-induced electron/energy transfer (PET),[4] metal−ligand charge transfer (MLCT),[5] intramolecular charge transfer (ICT),[6] excimer/exciplex formation,[7] excited state twisted intramolecular charge transfer (TICT),[8] and excited-state intra/intermolecular proton transfer (ESIPT).[9] However, these signaling mechanisms involve *the excited state* properties of the chemosensor prior to interaction with guest ions. In practicality, incorporation of such mechanisms in designing new fluorescent sensors has proven very unpredictable. It is therefore highly desirable to discover a useful and new design strategy for fluorescent sensors based on a relatively straightforward concept.

Pursuant to this, Wu et al. recently attempted to establish a new concept to amplify the fluorescence upon complexation with Zn^{2+}, whereby C═N isomerization was inhibited in an iminocoumarin system,[10] as it is well-known that the conjugated

*To whom correspondence should be addressed. E-mail: jinylee@skku.edu (J.Y.L.), jongskim@korea.ac.kr (J.S.K.).

(1) Reagan, M.; Bagchi, P.; Sumalekshmy, M.; Fahmi, C. J. *Chem. Rev.* **2009**, *109*, 4780.
(2) Johnson, A. R.; Munoz, A.; Gottlieb, J. L.; Jarrard, D. F. *J. Urol* . **2009**, *177*, 639.
(3) (a) de Silva, A. P.; Gunaratne, H. Q. N.; Gunnlaugsson, T.; Huxley, A. J. M.; McCoy, C. P.; Rademacher, J. T.; Rice, T. E. *Chem. Rev.* **1997**, *97*, 1515. (b) Kim, J. S.; Quang, D. T. *Chem. Rev.* **2007**, *107*, 3780. (c) Kim, H. N.; Lee, M. H.; Kim, H. J.; Kim., J. S.; Yoon, J. *Chem. Soc. Rev.* **2008**, *37*, 1465. (d) Senthilvelan, A.; Ho, I.-T.; Chang, K.-C.; Lee, G.-H.; Liu, I.-H.; Chung, W.-S. *Chem.—Eur. J.* **2009**, *15*, 6152. (e) Domaille, D. W.; Que, E. L.; Chang, C. J. *Nat. Chem. Biol.* **2008**, *4*, 168.
(4) (a) Aoki, I.; Sakaki, T.; Shinkai, S. *J. Chem. Soc., Chem. Commun.* **1992**, 730. (b) Kim, S. K.; Lee, S. H.; Lee, J. Y.; Bartsch, R. A.; Kim, J. S. *J. Am. Chem. Soc.* **2004**, *126*, 16499. (c) Chang, K.-C.; Su, I.-H.; Senthilvelan, A.; Chung, W.-S. *Org. Lett.* **2007**, *9*, 3363.
(5) (a) Jung, H. S.; Kwon, P. S.; Lee, J. W.; Kim, J. I.; Hong, C. S.; Kim, J. W.; Yan, S.; Lee, J. Y.; Lee, J. H.; Joo, T.; Kim, J. S. *J. Am. Chem. Soc.* **2009**, *131*, 2008. (b) Beer, P. D.; Drew, M. G. B.; Hesek, D.; Shade, M.; Szemes, F. *Chem. Commun.* **1996**, 2161.
(6) (a) Wang, J. B.; Qian, X. F.; Cui, J. N. *J. Org. Chem.* **2006**, *71*, 4308. (b) Coskun, A.; Akkaya, E. U. *J. Am. Chem. Soc.* **2005**, *127*, 10464. (c) Chen, C.-T.; Huang, W.-P. *J. Am. Chem. Soc.* **2002**, *124*, 6246. (d) Kim, S. K.; Bok, J. H.; Bartsch, R. A.; Lee, J. Y.; Kim, J. S. *Org. Lett.* **2005**, *7*, 4839. (e) Srikun, D.; Miller, E. W.; Domaille, D. W.; Chang, C. J. *J. Am. Chem. Soc.* **2008**, *130*, 4596. (f) Domaille, D. W.; Zeng, L.; Chang, C. J. *J. Am. Chem. Soc.* **2010**, *132*, 1194.
(7) (a) Wu, J.-S.; Zhou, J.-H.; Wang, P.-F.; Zhang, X.-H.; Wu, S.-K. *Org. Lett.* **2005**, *7*, 2133. (b) Jung, H. S.; Park, M.; Han, D. Y.; Kim, E.; Lee, C.; Ham, S.; Kim, J. S. *Org. Lett.* **2009**, *11*, 3378.
(8) Aoki, S.; Kagata, D.; Shiro, M.; Takeda, K.; Kimura, E. *J. Am. Chem. Soc.* **2004**, *126*, 13377.
(9) Sengupta, P. K.; Kasha, M. *Chem. Phys. Lett.* **1979**, *68*, 382.
(10) Wu, J.-S.; Liu, W.-M.; Zhuang, X.-Q.; Wang, F.; Wang, P.-F.; Tao, S.-L.; Zhang, X.-H.; Wu, S.-K.; Lee, S.-T. *Org. Lett.* **2007**, *9*, 33.

Published on Web 08/24/2010
© 2010 American Chemical Society

Scheme 1. Synthetic Pathways to **IC1**−**IC3** [a] and Their Crystal Structures[b]

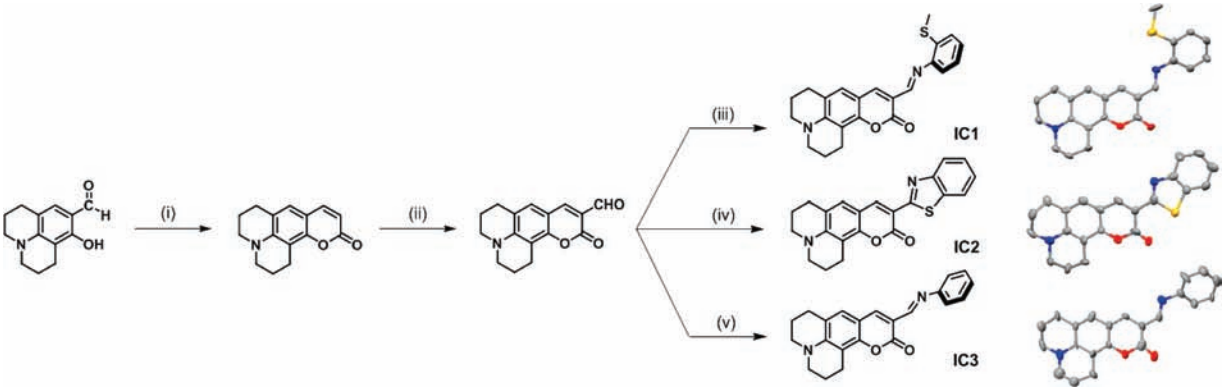

[a] Reagents and conditions: (i) $CH_2(COOC_2H_5)_2$, HCl/AcOH; (ii) $POCl_3$, DMF; (iii) 2-(metylthio)aniline, EtOH; (iv) 2-aminobenzenethiol, EtOH; (v) Aniline, EtOH. [b] All hydrogen atoms are omitted for clarity. Thermal ellipsoids are shown at the 50% probability level. Crystallographic data have been deposited with the Cambridge Crystallographic Data Centre under CCDC 763946 (**IC1**), 763947 (**IC2**), and 763948 (**IC3**).

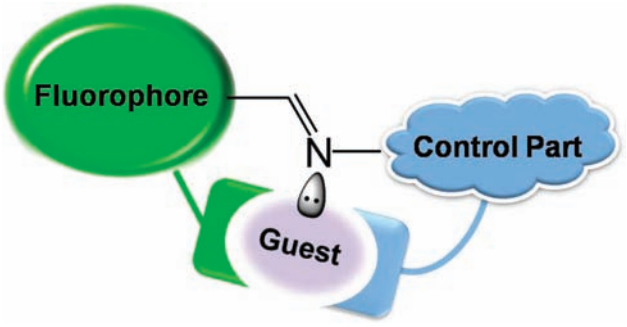

Figure 1. Conceptual architecture for the fluorescent sensors.

nitrogen lone pair electron at the α-[11] or *β*-positions[12] of the fluorophore is responsible for fluorescence quenching. Recently, Lippard and co-workers reported NO detection by fluorescence turn-on using Cu^{2+} complexes, where the nitrogen lone pair orbital plays an important role.[13] They observed remarkably enhanced fluorescence when the nitrogen lone pair orbital energy was greatly lowered by NO coordination.

As part of our research projects, these findings have prompted us to generate a new interaction mechanism for fluorescence enhancement utilizing the nitrogen lone pair for the next generation of sensors.

Results and Discussion

The conceptual architecture is depicted in Figure 1 where the -C═N- is located in conjunction with a fluorophore and a control part at a position *β* to the -C═N-. The C═N group was chosen so as to take advantage of the C═N isomerization, as well as the PET phenomenon in fluorescence. The nitrogen lone pair electron was expected to contribute to the fluorescence, which could be tuned by modifying the control part or by the metal coordination. In the present study, a coumarin moiety was selected as the fluorophore as it is a widely accepted fluorophore in detection of trace elements (Cu^{2+}, Zn^{2+}) in biological systems with high quantum yield and comparatively lower toxicity.[5a,14] The methyl aryl thioether was adapted as the controlling part. For fluorescence tuning, such as modulating the nitrogen lone pair orbital contribution, two different approaches were adapted: (i) cyclization of the controlling part into the C═N; (ii) Zn^{2+} coordination to block the nitrogen lone pair orbital.

The **IC1** (hereafter **IC** represents iminocoumarin) and its analogues were rationally designed and synthesized with unique features to demonstrate the fluorescence intensity changes dependent on the geometry and participation of the imine lone pair electrons as proposed. Compounds **IC1**−**IC3** were synthesized in high yields as shown in Scheme 1. Purposely, the $-SCH_3$ group was introduced at the *o*-position of the aryl imine as a possible binding site with metal ions in the **IC1**; nevertheless, the **IC3** analogue bore an open structure without addition of a binding site, and the **IC2** analogue was a complete planar cyclic structure, as shown in Scheme 1. Single crystals of **IC1**−**IC3** were grown under vapor diffusion of ethyl ether into CH_3CN (Scheme 1). The C═N−C−C dihedral angle was 145.4°, which revealed the twist *s-trans* conformation of **IC1**, whereas **IC2** was planar (−177.0°).

Compounds **IC1** and **IC2** show UV absorption centered at 475 and 477 nm, respectively (Supporting Information, Figure S1), implying absorption of UV light independent of ligand planarity. However, twisted nonplanar **IC1** and **IC3** showed very low fluorescence signal with quantum yields of $\Phi_f = 0.01$, whereas planar **IC2** showed strong green fluorescence at $\lambda_{max} = 518$ nm, with a quantum yield (Φ_f) of 0.79 (Figure 2 and Table 1). The remarkably high fluorescence in **IC2**, compared to **IC1**, is due to blocking of the nitrogen lone pair orbital contribution to the excitation by cyclization of the C═N group; hence, the nitrogen lone pair orbital is prevented from fluorescence quenching (vide infra). This phenomenon provokes the possibility of *fluorescence enhancement by orbital control* (**FEOC**). Although the main origin of the fluorescence

(11) (a) Iyoshi, S.; Taki, M.; Yamamoto, Y. *Inorg. Chem.* **2008**, *47*, 3946. (b) Parkesh, R.; Lee, T. C.; Gunnlaugsson, T. *Org. Biomol. Chem.* **2007**, *5*, 310.

(12) (a) Xue, L.; Liu, C.; Jiang, H. *Org. Lett.* **2009**, *11*, 1655. (b) Bazzicalupi, C.; Bencini, A.; Biagini, S.; Bianchi, A.; Faggi, E.; Giorgi, C.; Marchetta, M.; Totti, F.; Valtancoli, B. *Chem.—Eur. J.* **2009**, *15*, 8049. (c) Moore, E. G.; Bernhardt, P. V.; Furstenberg, A.; Riley, M. J.; Smith, T. A.; Vauthey, E. *J. Phys. Chem. A* **2005**, *109*, 3788. (d) Burdette, S. C.; Walkup, G. K.; Spingler, B.; Tsien, R. Y.; Lippard, S. J. *J. Am. Chem. Soc.* **2001**, *123*, 7831. (e) Burdette, S. C.; Frederickson, C. J.; Bu, W. M.; Lippard, S. J. *J. Am. Chem. Soc.* **2003**, *125*, 1778. (f) Kulatilleke, C. P.; de Silva, S. A.; Eliav, Y. *Polyhedron* **2006**, *25*, 2593. (g) Xue, L.; Wang, H. H.; Wang, X. J.; Jiang, H. *Inorg. Chem.* **2008**, *47*, 4310.

(13) Lim, M. H.; Wong, B. A.; Pitcock, W. H.; Mokshagundam, D.; Baik, M. H.; Lippard, S. J. *J. Am. Chem. Soc.* **2006**, *128*, 14364.

(14) Komatsu, K.; Urano, Y.; Kojima, H.; Nagano, T. *J. Am. Chem. Soc.* **2007**, *129*, 13447.

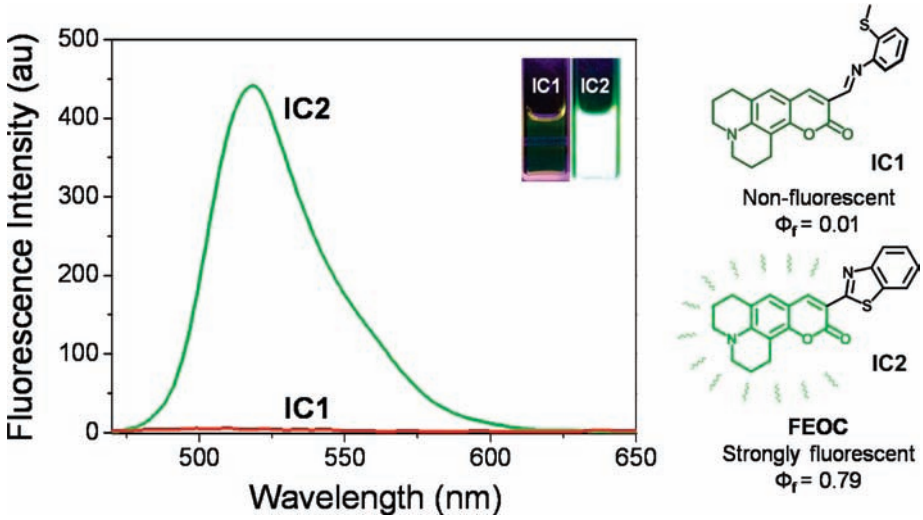

Figure 2. Fluorescence spectra (excited at 500 nm) of **IC1** and **IC2** (10 μM) in CH_3CN solution.

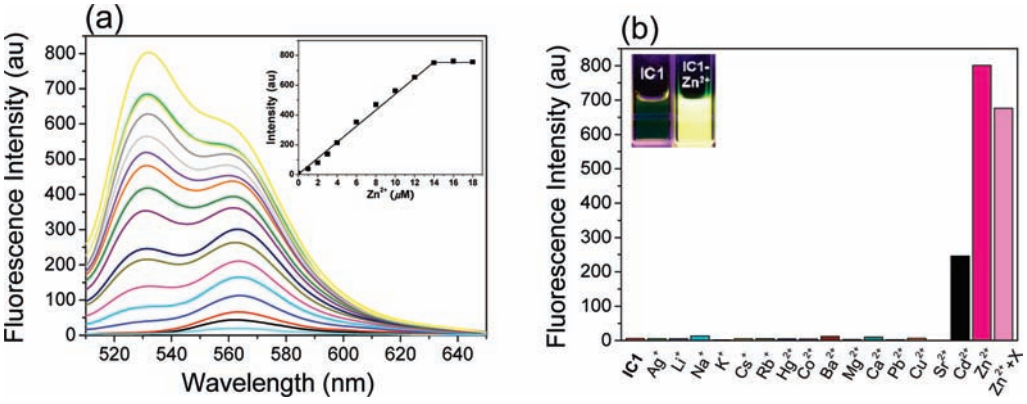

Figure 3. (a) Fluorescence emission spectra of **IC1** (10 μM) with various concentrations of $Zn(ClO_4)_2$ [0−1.4 equiv, respectively]; (b) Histogram of **IC1** (10 μM) upon addition of ClO_4^- salts of Ag^+, Li^+, Na^+, K^+, Cs^+, Rb^+, Hg^{2+}, Co^{2+}, Ba^{2+}, Mg^{2+}, Ca^{2+}, Pb^{2+}, Cu^{2+}, Sr^{2+}, Cd^{2+}, Zn^{2+}, and Zn^{2+} + X (other all metals) (10 equiv, respectively) in CH_3CN with excitation at 500 nm. (Bars indicate the fluorescence ratio at 532 nm emission). The inset shows the correlation between the fluorescence intensity and zinc concentration.

Table 1. Photophysical Data[α]

compound	absorbance max (nm)	emission max (nm)	relative quantum yield (Φ_f)
IC1	475	509	0.01
IC2	477	518	0.79
IC3	474	508	0.01
IC1 + Zn^{2+}	504	530	0.39

[α] Φ_f: Relative Fluorescence Quantum Yield (fluorescein in 0.1N NaOH as a reference, Φ_f = 0.85).[15]

mechanism in this study is basically PET (photoinduced electron transfer),[3a,b] we here propose the new terminology **FEOC** with which one easily guesses the nitrogen lone pair orbital contribution in the molecular structure rather than the PET contribution. With only conventional PET, the high quantum yield of **IC2** cannot be properly explained. However, the concept of **FEOC** can be explained in the non-chelating systems as shown in **IC2** as well as in the chelating systems. Thus, we ensure that **FEOC** is more general concept than conventional CHEF.

To gain insight into the metal ion binding effects upon the fluorescence behavior of **IC1**, various cations were added to the acetonitrile solution to give a noticed and remarkable fluorescence enhancement (~4,100%) upon binding with Zn^{2+} ions over other transition and post-transition metal ions, as shown in Figure 3. Only Cd^{2+} shows an obvious fluorescence change (~820%). The alkali metal ions were unable to improve any fluorescence signal as they have feeble bonding affinity toward the C=O and −S−Me groups.[10] Simultaneously, the UV absorption is slightly red-shifted to 504 from 475 nm (Supporting Information, Figure S2) and reaches saturation at 1.0 equiv of Zn^{2+}, implicating a 1:1 complexation of ligand with the Zn^{2+} ion. The quantum yield of **IC1** in CH_3CN is also enhanced upon binding with the Zn^{2+} ion by a factor of 39, compared with **IC1** alone (Table 1). To understand the complexation ratio of Zn^{2+} with **IC1**, a Job's plot analysis was performed (Supporting Information, Figure S3) and the FAB mass spectrum (Supporting Information, Figure S4) of **IC1-Zn^{2+}** complex recorded; both experimental data indicates a 1:1 complex of **IC1** with Zn^{2+}. The corresponding calculated association constant of **IC1** for Zn^{2+} was $1.21 \pm 0.03 \times 10^6$ M^{-1}.[16] Fortunately, obtainment

(15) Paeker, A.; Rees, W. T. *Analyst* **1960**, *85*, 587.

(16) (a) Haugland, R. P. *Handbook of Fluorescent Probes and Research Products*, 10th ed.; Molecular Probes, Inc.: Eugene, OR, 2005. (b) Association constants were obtained using the computer program ENZFITTER, available from Elsevier-BIOSOFT, 68 Hills Road, CambridgeCB2 1LA, U.K. (c) Connors, K. A. *Binding Constants*; Wiley: New York, 1987.

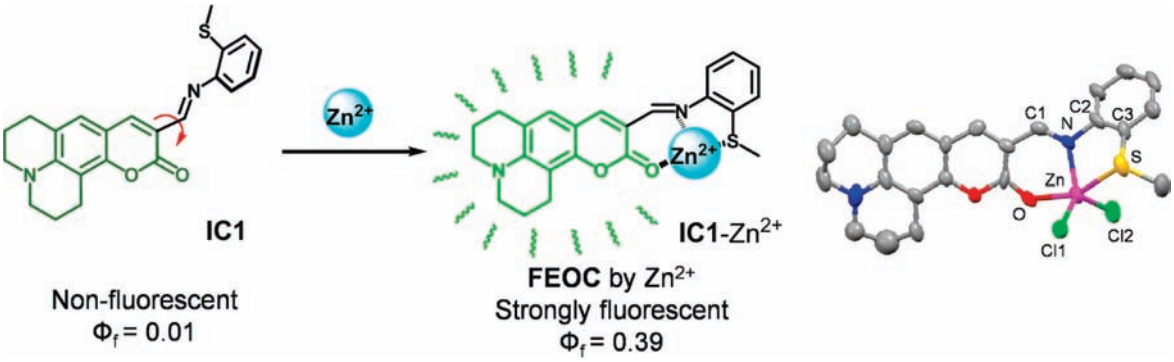

Figure 4. Quantum yield change of **IC1** by Zn^{2+} coordination and its crystal structure of the complex. Thermal ellipsoids are shown at the 50% probability level. Hydrogen atoms are omitted for clarity. Select bond lengths (Å) and dihedral angles (deg): Zn−O 2.163; Zn−N 2.120; Zn−S 2.748; Zn−Cl1 2.244; Zn−Cl2 2.205; C1−N−C2−C3 143.8(0). The crystallographic data have been deposited with the Cambridge Crystallographic Data Centre under CCDC 763945.

of a crystal structure of **IC1-Zn^{2+}** complex (Figure 4) indicated that the C1=N−C2−C3 dihedral angle was slightly reduced to 143.8°, with retainment of the *s-trans* configuration. This structural information suggests that fluorescence enhancement of **IC1** by Zn^{2+} coordination does not originate from planarity or C−C rotation as previously reported.[6] Instead, the lone pair electrons of the imine nitrogen may play a pivotal role in fluorescent amplification, which strongly suggests the possibility of *fluorescence enhancement by orbital control* (**FEOC**). A similar experiment was performed for **IC3**. There was, however, no significant change in fluorescent signal upon addition of various ions (Supporting Information, Figure S5), suggesting that the *o*-methylthio unit only plays an important role in complexation with Zn^{2+} in **IC1**.

In addition, another experiment was carried out to understand the practical ability of **IC1** to sense the Zn^{2+} ions in the presence of other interfering metal ions (Ag^{+}, Li^{+}, Na^{+}, K^{+}, Rb^{+}, Cs^{+}, Hg^{2+}, Co^{2+}, Ba^{2+}, Mg^{2+}, Ca^{2+}, Pb^{2+}, Cu^{2+}, Sr^{2+}, Cd^{2+}). From this, there is a remarkable fluorescent increment (Supporting Information, Figure S6) but little suppression. We have also checked the anion effects with various anions in presence of Zn^{2+} and found some anion effects of **IC1** from UV absorption and fluorescence spectra (Supporting Information, Figure S7). It is probably due to their ionic strength differences or different coordination mode when they are ligated by ionofluorophores.

To validate the experimental observations, quantum calculations were executed to verify the fluorescence behavior of **IC1**, analogue **IC2**, and the chelating complex **IC1-Zn^{2+}**. The density functional theory (DFT) calculations were performed using a B3LYP exchange functional with 6-31G* basis sets employing a suite of Gaussian 03 programs.[17] The calculated lowest energy structures are shown in Supporting Information, Figure S8. In **IC1**, the methyl phenyl thioether group is significantly tilted with the coumarin moiety, while in **IC2**, it is almost planar through the cyclization. The most striking structural feature of **IC1** in the Zn^{2+} coordination is the turning of the methyl phenyl thioether group such that the sulfur atom is involved in the Zn^{2+} coordination together with the nitrogen, oxygen, and two chloride atoms. The calculated dihedral angles of **IC1**, **IC2**, and **IC1-Zn^{2+}** were in good agreement with the experimental crystal structures, as shown in Supporting Information, Table S1, Scheme 1, and Figure 4. The planar conformation is highly stabilized with the resonance electron delocalization; thus, in **IC2**, conformational isomerization is almost forbidden.

To further investigate the fluorescence behavior of **IC1**, **IC2**, and **IC1-Zn^{2+}**, time-dependent DFT (TDDFT) calculations were also carried out. The excited state calculations with TDDFT resulted in oscillator strengths of 0.596, 1.024, and 0.649, and respective absorption wavelengths of 393.0, 406.0, and 413 nm for **IC1**, **IC2**, and **IC1-Zn^{2+}**. The calculated wavelengths were consistent with experimental values and within 60−70 nm deviations, due possibly to solvent effects. The origin of the fluorescence in **IC1**, **IC2**, and **IC1-Zn^{2+}** can be fully understood based on the nitrogen orbital action. The molecular orbitals relevant to the most dominant electronic oscillators to the absorption for **IC1**, **IC2**, and **IC1-Zn^{2+}** are shown in Supporting Information, Figure S9 and S10.

Importantly, Figure 5 shows the energy levels of the frontier molecular orbitals, including the nitrogen lone pair orbitals of **IC1**, **IC2**, and **IC1-Zn^{2+}**, and the electronic configurations of the ground and excited states. In **IC1**, the contribution of the nitrogen lone pair orbital (HOMO-1) to the excitation is 90%, subsequently causing fluorescence quenching. However, in **IC2**, the nitrogen lone pair orbital (HOMO-4) does not participate in the excitation, thus, no fluorescence quenching. It should be noted that in the case of **IC1**, the HOMO-1 energy (−5.442) was slightly lower than the highest occupied molecular orbital (HOMO) energy (−5.034); furthermore, in **IC2**, the HOMO-4 energy (−7.184) was much lower than the HOMO energy (−5.197). Hence, the nitrogen lone pair orbital is not involved in the excitation because of the large stabilization of its lone pair orbital. Nevertheless, when Zn^{2+} is coordinated to **IC1**, the nitrogen lone pair orbital has a strong interaction with Zn^{2+} d-orbitals to produce a bonding type (HOMO-6) and antibonding type (HOMO-4) orbital (Figure 5 and Supporting Information, Figure S8). The energies of the HOMO-6 and HOMO-4 are −6.748 and −6.150, lower than the HOMO energy (−5.714). The nitrogen lone pair orbitals (HOMO-6 and HOMO-4) are not involved in the excitation, instead HOMO (8%), HOMO-1 (44%), HOMO-2 (8%), HOMO-3 (17%), and HOMO-5 (23%) were involved; thus, the nitrogen lone pair orbital does not have a quenching effect in **IC1-Zn^{2+}**. It should be noted that this is quite different from the case of **IC2** in that the nitrogen lone pair orbital has no contribution, mainly because of the energy lowering in **IC2**, while in **IC1-Zn^{2+}**, the HOMO-5 is lower lying than the nitrogen lone pair orbital (HOMO-4) that contributed 23% to the excitation. Thus, the blocking of the nitrogen lone pair orbital, and hence the

(17) Kim, H. J.; Bhuniya, S.; Mahajan, R. K.; Puri, R.; Liu, H.; Ko, K. C.; Lee, J. Y.; Kim, J. S. *Chem. Commun.* **2009**, 7128.

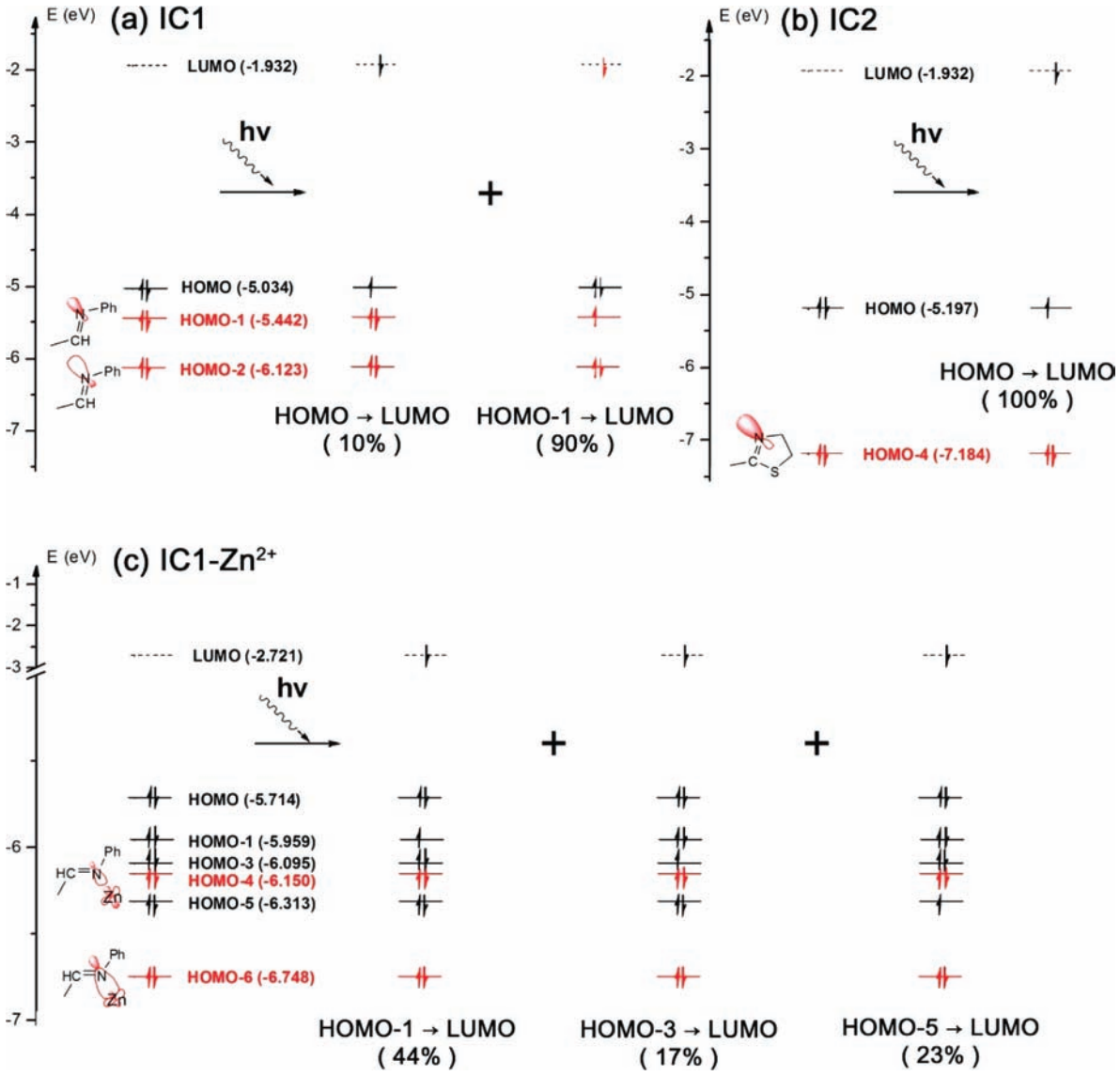

Figure 5. Energy levels of the frontier molecular orbitals of **IC1**, **IC2**, and **IC1-Zn^{2+}**.

fluorescence enhancement, can be achieved not only by cyclization (**IC2**) but also by metal coordination as well (**IC1-Zn^{2+}**).

The quantum calculations revealed that fluorescent amplification of **IC1** upon binding with Zn^{2+} ions was due to the blocking of nitrogen lone pair electrons rather than conformational change or attained planarity of the complex. This is supportive of the prediction proffered herein, namely, the possibility of *fluorescence enhancement by orbital control* (**FEOC**).

Conclusions

We have devised a new strategy to generate new fluorescent sensors based on nitrogen lone pair orbital control, referred to as *fluorescence enhancement by orbital control* (**FEOC**). Accordingly, newly synthesized coumarin derivatives are unique examples of this category. In **IC1**, the fluorescence quenching was dominant because of the nitrogen lone pair orbital contribution to the excitation, while **IC2** gave a remarkable fluorescence enhancement because of the blocking of the nitrogen lone pair orbital contribution by cyclization and partly because of the planarity and isomerization blocking. However, upon Zn^{2+} coordination, the **IC1** showed a significant fluorescence enhancement not due to the geometrical factor, but rather the blocking of the nitrogen lone pair orbital by metal coordination. We therefore believe that this new concept will be widely used in the future to design fluorescence turn-on sensors based on orbital control.

Experimental Section

General Information and Materials. All fluorescence and UV/vis absorption spectra were recorded in a Shimadzu RF-5301PC and a Shinco S-3100 spectrophotometer, respectively. NMR and mass spectra were recorded at Varian instrument (400 MHz) and JMS-700 MStation mass spectrometer, respectively. All reagents and cationic compounds such as perchlorate of Ag^{+}, Li^{+}, Na^{+}, K^{+}, Cs^{+}, Rb^{+}, Hg^{2+}, Co^{2+}, Ba^{2+}, Mg^{2+}, Ca^{2+}, Pb^{2+}, Cu^{2+}, Sr^{2+}, Cd^{2+}, Zn^{2+} were purchased from Aldrich and used as received.

General Procedure for the Syntheses.

Compound IC1. A portion of iminocoumarin aldehyde[18] (269 mg, 1.0 mmol) and 2-(methylthio)aniline (195 mg, 1.4 mmol) was combined in absolute ethanol (10 mL) to yield a transient scarlet precipitate. The solution was stirred under reflux for 4 h,

(18) Lim, N. C.; Schuster, J. V.; Porto, M. C.; Tanudra, M. A.; Yao, L.; Freake, H. C.; Brückner, C. *Inorg. Chem.* **2005**, *44*, 2018.

and the precipitate was filtrated, washed with absolute ethanol three times, and recrystallized from C_2H_5OH to yield yellow crystals (**IC1**, 320.2 mg, 0.82 mmol) in 82% yield. Mp: 170−172 °C; TLC (EtOAc:*n*-hexane, 1:1 v/v): R_f = 0.12; ^{1}H NMR (400 MHz, $CDCl_3$): δ 8.68 (s, 1H), 8.51 (s, 1H), 7.20−7.18 (m, 2H), 7.17−7.12 (m, 1H), 7.06−7.04 (m, 1H), 7.02 (s, 1H), 3.33 (q, J = 5.62 Hz, 4H), 2.91 (t, J = 6.42 Hz, 2H), 2.78 (t, J = 4.00 Hz, 2H), 2.46 (s, 3H), 1.99 (m, 4H); ^{13}C NMR (100 MHz, $CDCl_3$): 163.0, 154.8, 152.9, 149.2, 147.8, 142.1, 134.5, 127.3, 126.6, 125.4, 124.3, 119.5, 118.0, 114.2, 109.0, 106.5, 50.5, 50.1, 27.7, 21.5, 20.6,20.4,15.0. FAB-MS calc. for $C_{23}H_{22}N_2O_2S$ $[M+H]^+$ 391.1, found 391.4. Anal. Calcd for $C_{23}H_{22}N_2O_2S \cdot 0.2CH_2Cl_2$: C, 68.38; H, 5.55, Found: C, 68.48; H, 5.23.

Compound IC2. Synthetic procedures are similar to that of **IC1** to give 318.3 mg, 0.85 mmol in 85% yield. Mp: 190 °C; TLC (EtOAc:*n*-hexane, 1:3 v/v): R_f = 0.3; ^{1}H NMR (400 MHz, $CDCl_3$): δ 8.80 (s, 1H), 8.00 (d, J = 8.30 Hz, 1H), 7.93 (d, J = 7.84 Hz, 1H), 7.47 (t, J = 8.53 Hz, 1H), 7.35 (t, J = 8.30 Hz, 1H), 7.05 (s, 1H), 3.36−3.29 (m, 4H), 2.94 (t, J = 7.58 Hz, 2H), 2.79 (t, J = 7.17 Hz, 2H), 2.03−1.94 (m, 4H). ^{13}C NMR (100 MHz, $CDCl_3$): 162.9, 154.9, 153.0, 149.2, 147.9, 142.1, 134.5, 127.4, 126.5, 125.5, 124.4, 119.5, 118.0, 114.2, 109.1, 106.4, 50.5, 50.1, 27.7, 21.5, 20.6, 20.4, 15.0. FAB-MS calc. for $C_{22}H_{18}N_2O_2S$ $[M+H]^+$ 375.1, found 375.2. Anal. Calcd for $C_{22}H_{18}N_2O_2S \cdot 0.25CH_2Cl_2$: C, 67.53; H, 4.72, Found: C, 67.59; H, 4.53.

Compound IC3. Synthetic procedures are similar to that of **IC1** to give 275.5 mg, 0.80 mmol in 80% yield. Mp: 168 °C; TLC (EtOAc:*n*-hexane, 1:1 v/v): R_f = 0.14; ^{1}H NMR (400 MHz, $CDCl_3$): δ 8.72 (s, 1H), 8.42 (s, 1H), 7.37 (t, J = 7.94 Hz, 2H), 7.24 (m, 3H), 6.98 (s, 1H), 3.33 (q, J = 5.62 Hz, 4H), 2.91 (t, J = 6.42 Hz, 2H), 2.78 (t, J = 4.00 Hz, 2H), 1.99 (m, 4H). ^{13}C NMR (100 MHz, $CDCl_3$): 162.8, 155.2, 152.7, 151.9, 147.7, 141.3, 129.2, 126.9, 125.9, 121.2, 119.3, 114.0, 108.6, 106.2, 50.2, 49.8, 29.7, 27.5, 21.2, 20.3, 20.2; FAB-MS calc. for $C_{22}H_{20}N_2O_2$ $[M+H]^+$ 345.2, found 345.3. Anal. Calcd for $C_{22}H_{20}N_2O_2 \cdot 0.6CH_3OH$: C, 74.64; H, 6.22, Found: C, 74.71; H, 6.67.

Spectroscopic Data. Stock solutions (1.00 mM) of the metal perchlorate salts were prepared in CH_3CN. Stock solutions of **IC1**−**IC3** (0.3 mM) were prepared in CH_3CN. For all measurements of fluorescence spectra, excitation was at 500 nm with excitation and emission slit widths at 1.5 nm. UV/vis and fluorescence titration experiments were performed using 10 μM of **IC1**−**IC3** in CH_3CN with varying concentrations of the metal perchlorate salts. After calculating the concentrations of the free ligand and the complexed form of **IC1** from the fluorescence titration experiments, the association constants were obtained using the computer program ENZFITTER.[16]

Calculation Details. All theoretical calculations were carried out within the density functional theory (DFT) approach using a suite of Gaussian 03 programs.[19] Geometry optimizations were performed using Becke's three-parameter B3LYP exchange-correlation functional[20] and the 6-31G* basis set.[21] Then, at the optimized geometries, the time- dependent density functional theory (TDDFT) calculations were performed to obtain their excitation properties (transition energies and oscillator strengths).

Acknowledgment. This work was supported by the CRI program (No. 2010-0000728) from National Research Foundation of Korea (J.S.K.). J.Y.L. acknowledges the NRF grants (No. 20100001630) and (KRF-2008-313-C00388) funded by MEST.

Supporting Information Available: X-ray crystallographic data for **IC1**, **IC2**, **IC3**, and **IC1**-Zn^{2+} in CIF format. UV−vis absorption spectra (Figures S1−S2). Fluorescence spectra (Figures S5−S6). Calculation (Table S1, Figures S8−S10). NMR and Mass spectrometry spectra for all compounds (Figures S11−S19). This material is available free of charge via Internet at http://pubs.acs.org.

(19) Frisch, M. J.; Trucks, G. W.; Schlegel, H. B.; Scuseria, G. E.; Robb, M. A.; Cheeseman, J. R.; Montgomery, Jr., J. A.; Vreven, T.; Kudin, K. N.; Burant, J. C.; Millam, J. M.; Iyengar, S. S.; Tomasi, J.; Barone, V.; Mennucci, B.; Cossi, M.; Scalmani, G.; Rega, N.; Petersson, G. A.; Nakatsuji, H.; Hada, M.; Ehara, M.; Toyota, K.; Fukuda, R.; Hasegawa, J.; Ishida, M.; Nakajima, T.; Honda, Y.; Kitao, O.; Nakai, H.; Klene, M.; Li, X.; Knox, J. E.; Hratchian, H. P.; Cross, J. B.; Bakken, V.; Adamo, C.; Jaramillo, J.; Gomperts, R.; Stratmann, R. E.; Yazyev, O.; Austin, A. J.; Cammi, R.; Pomelli, C.; Ochterski, J. W.; Ayala, P. Y.; Morokuma, K.; Voth, G. A.; Salvador, P.; Dannenberg, J. J.; Zakrzewski, V. G.; Dapprich, S.; Daniels, A. D.; Strain, M. C.; Farkas, O.; Malick, D. K.; Rabuck, A. D.; Raghavachari, K.; Foresman, J. B.; Ortiz, J. V.; Cui, Q.; Baboul, A. G.; Clifford, S.; Cioslowski, J.; Stefanov, B. B.; Liu, G.; Liashenko, A.; Piskorz, P.; Komaromi, I.; Martin, R. L.; Fox, D. J.; Keith, T.; Al-Laham, M. A.; Peng, C. Y.; Nanayakkara, A.; Challacombe, M.; Gill, P. M. W.; Johnson, B.; Chen, W.; Wong, M. W.; Gonzalez, C.; and Pople, J. A. *Gaussian 03*, revision C02; Gaussian Inc.: Pittsburgh, PA, 2004.

(20) (a) Lee, C.; Yang, W.; Parr, R. G. *Phys. Rev. B* **1988**, *37*, 785. (b) Becke, A. D. *J. Chem. Phys.* **1993**, *98*, 5648.

(21) Hehre, W. J.; Ditchfield, R.; Pople, J. A. *J. Chem. Phys.* **1972**, *56*, 2257.